

Fig. 3 by inverting the time-dependent orbital energy  $E_A(\Delta)$  into time-dependent position  $R_{\text{Cu-Cs}}(\Delta)$  via the calculated dependence of the  $6s+6p_z$  orbital energy on  $R_{\text{Cu-Cs}}$  (13). A fit of  $R_{\text{Cu-Cs}}(\Delta)$  to a fourth-order polynomial gives a continuous function  $R(\Delta)$ , which is differentiated to obtain the acceleration of Cs atoms  $a=\partial^2R(\Delta)/\partial\Delta^2$ . The force acting on Cs atoms,  $F=ma$ , is then integrated,  $U=-\int FdR$ , to derive the experimental PES (Fig. 4C). This classical model explains the unusual nonexponential decay of the antibonding state in terms of a stretching of the Cu–Cs bond by  $\sim 0.35$  Å within 160 fs of the excitation (18).

Although the Cu–Cs bond elongation is considerable, the most probable outcome of the photoexcitation is electronic relaxation back to the ground state. The desorption yield can be estimated from an increase in the work function  $\Phi$  due to a photoinduced decrease of the Cs coverage (19), which gives an upper limit for the photodesorption cross section  $\sigma_{\text{Cs/Cu}}$  of  $2.4 \times 10^{-23}$  cm<sup>2</sup>. By contrast, the cross section for desorption of K from graphite  $\sigma_{\text{K/C}}$  is  $2 \times 10^{-20}$  cm<sup>2</sup> (5). These two chemisorption systems probably have similar excitation probabilities and excited state lifetimes (5), and such a large difference in the cross sections must therefore arise from both different PES topologies and nuclear masses. This conclusion is consistent with the experimentally derived PES, which is much less repulsive at the point of excitation for Cs/Cu(111) than for K/C. Furthermore, the present one-dimensional model does not consider the recoil motion of substrate Cu atoms, which will lead to a significant transfer of energy to bulk phonons. These differences imply that photoexcitation imparts less velocity to Cs than to K, making its chance of escape much smaller for a comparable lifetime.

A possible extension of these results is to apply the photoinduced displacement of alkali atoms in an ultrafast atomic switch. Eigler demonstrated a switch based on reversible transfer of Xe atoms between a Ni(110) surface and a scanning tunneling microscope (STM) tip (20). A plausible mechanism for the transfer is vibrational heating through multiple cycles of excitation and relaxation involving electron scattering through the unoccupied  $6s$  orbital of Xe (21). Because of the limited excitation rate and inelastic scattering probability, however, the Eigler switch is inherently slow (on the order of a nanosecond). Femtosecond-length laser excitation could also actuate alkali atom transfer in a surface-STM junction. The chemisorption strength of Cs and excited-state distension are adequate to induce transfer in a single photoexcitation step. With a  $<200$ -fs transfer time, such a device could be many orders of magnitude faster and more efficient than the Eigler switch.

The possibility of resolving the nuclear motion of atoms and molecules on surfaces at

femtosecond and angstrom scales through time-resolved photoemission spectroscopy has been demonstrated. Recent studies of other alkali atom adsorbates and noble metal substrates suggest that Cs/Cu(111) is not unique (16). Systematic studies of other systems will lead to a more complete understanding of the principles involved in the electronic relaxation, desorption, and atomic manipulation of metal surfaces.

References and Notes

1. H.-L. Dai and W. Ho, Eds., *Laser Spectroscopy and Photochemistry on Metal Surfaces*, vol. 5 (World Scientific, Singapore, 1995).
2. D. Menzel and R. Gomer, *J. Chem. Phys.* **41**, 3311 (1964).
3. L. Bartels *et al.*, *Phys. Rev. Lett.* **80**, 2004 (1998).
4. F. M. Zimmermann and W. Ho, *Surf. Sci. Rep.* **22**, 127 (1995).
5. B. Hellsing, D. V. Chakarov, L. Österlund, V. P. Zhadanov, B. Kasemo, *J. Chem. Phys.* **106**, 982 (1996).
6. H. Petek and S. Ogawa, *Prog. Surf. Sci.* **56**, 239 (1997).
7. U. Höfer *et al.*, *Science* **277**, 1480 (1997).
8. N.-H. Ge *et al.*, *Science* **279**, 202 (1998).
9. S. Ogawa, H. Nagano, H. Petek, *Phys. Rev. Lett.* **82**, 1931 (1999).
10. R. D. Diehl and R. McGrath, *J. Phys. Condens. Matter* **9**, 951 (1997).
11. A. M. Bradshaw, H. P. Bonzel, G. Ertl, *Physics and Chemistry of Alkali Metal Adsorption* (Elsevier, Amsterdam, 1989).
12. J. P. Muscat and D. M. Newns, *Surf. Sci.* **84**, 262 (1979).
13. A. G. Borisov, A. K. Kazansky, J. P. Gauyacq, *Surf. Sci.* **430**, 165 (1999).

14. H. Ishida and A. Liebsch, *Phys. Rev. B* **45**, 6171 (1992).
15. The excitation source is a frequency-doubled (3.08 eV) Ti:sapphire laser producing an 80-MHz train of 16-fs pulses with  $<0.5$  nJ energy. Delay between the pulse-pair is set within  $5 \times 10^{-17}$  s (1/25 of a cycle of 400-nm light) by a Mach-Zehnder interferometer. A single-crystal Cu(111) surface is covered under ultrahigh vacuum by 0.08 to 0.10 monolayer (ML) of Cs atoms (coverage  $\Theta_{\text{Cs}}$  of  $1.8 \times 10^{15}$  atoms/cm<sup>2</sup> corresponds to 1 ML), and cooled to 33 K.
16. H. Petek, M. J. Weida, H. Nagano, S. Ogawa, *Surf. Sci.* **451**, 22 (2000).
17. S. Ogawa, H. Nagano, H. Petek, *Surf. Sci.* **427/428**, 34 (1999).
18. Alternative explanations involving inhomogeneous effects leading to site- or energy-dependent antibonding state lifetimes are excluded for the following reasons: (i) A is homogeneously broadened, as reported in (17); (ii) although an inhomogeneous sample can result in multiexponential decay, it is difficult to construct a mechanism that could explain the observed nonexponential decay; (iii) the lifetime of A is independent of energy between 2.4 and 3.2 eV at 300 K [M. Bower, S. Pawlik, M. Aeschlimann, *Phys. Rev. B* **60**, 5016 (1999)]; and (iv) a quadratic dependence of  $E_A(\Delta)$  would be highly coincidental.
19. S. Ogawa, M. J. Weida, H. Nagano, H. Petek, unpublished data.
20. D. M. Eigler, C. P. Lutz, W. E. Rudge, *Nature* **352**, 600 (1991).
21. S. Gao, M. Persson, B. I. Lundqvist, *Solid State Commun.* **84**, 271 (1992).
22. We acknowledge N. Moriya, S. Matsunami, and S. Saito for technical support and NEDO for partial funding for this project through the International Joint Research Grant. M.J.W. thanks NSF and the Center for Global Partnership for support (NSF grant INT-9819100).

17 January 2000; accepted 4 April 2000

# Electron-Induced Inversion of Helical Chirality in Copper Complexes of *N,N*-Dialkylmethionines

Steffen Zahn and James W. Canary\*

Stereodynamic complexes of copper were found to undergo inversion of a helical chiral element upon oxidation or reduction. The amino acid methionine was derivatized by the attachment of two chromophores to the nitrogen atom. The resultant ligands formed stable complexes with Cu<sup>I</sup> and Cu<sup>II</sup> salts. For a derivative of a given absolute chirality, the complexes afford nearly mirror image circular dichroism spectra. The spectral changes originate from reorientation of the nitrogen-attached chromophores due to a conformation interconversion driven by the exchange of a carboxylate for a sulfide ligand. The electrically induced chirality inversion coupled with strong interactions with polarized light is unique and may lead to novel chiral molecular devices.

Manipulation of the handedness of molecular shape is an uncommon but potentially very useful phenomenon. Inversion of the helical chirality formed by aromatic substituents has been

achieved by photochemical isomerization of aryl-substituted alkenes (1–3) or by photochemical electrocyclic reactions (3). For systems that also show photochromism, reversible inversion of helical chirality may be achieved by monochromatic light. These studies have generated interest in molecular electronics applications, although one problem that has been encountered is destructive readout (4). Here, we

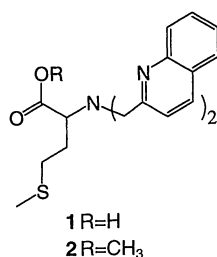
Department of Chemistry, New York University, New York, NY 10003, USA.

\*To whom correspondence should be addressed. E-mail: james.canary@nyu.edu

report a molecule that exhibits the inversion of an element of axial chirality upon a redox change. A number of interesting redox-induced changes in molecular geometry have been reported recently (5–11), including solid state applications (12). Redox switching was also observed recently by spectroelectrochemistry with circular dichroism (CD) detection (13, 14). To our knowledge, there have been no reports of inversion of molecular chirality by electrical means. Electrical inversion of molecular chirality and strong anisotropic interactions with light may be useful in the design of materials for applications in molecular electronics (12) or optical displays (15). Additionally, the changes in molecular conformation proposed for our system suggest new strategies for nanomechanical devices (16, 17).

Our approach to this problem grew out of our studies of conformationally biased, labile coordination complexes (18, 19) and methods for the determination of absolute configurations of amines (20). Central to these studies is the observation that tripodal ligands with a single chiral center in one of the arms experience a conformational bias affording an additional element of axial chirality (21). The adopted propeller-like conformation may fix the orientation of appended or inherent chromophores so that the electronic transitions can interact by a coupled oscillator mechanism, resulting in exciton-coupled circular dichroism (ECCD) (22, 23). In prior work, we showed that the ECCD spectral amplitude could be modulated by one-electron redox chemistry of copper ions (5), and we correlated the spectroscopic change with conformational dynamics of the ligand in Cu<sup>I</sup> and Cu<sup>II</sup> states. In essence, we were able to turn the CD signal “on” or “off” by the addition or removal of an electron from a copper ion. It then became of interest to find a way to invert the handedness of the propeller by inducing a change in the conformation of the ligand. Such an achievement would result in an electron-triggered “+/-” switch, which, to our knowledge, is not known outside of the present work.

It is well known that Cu<sup>II</sup> ions form very stable complexes with carboxylates, whereas Cu<sup>I</sup> favors sulfide ligands (24). It thus seemed plausible that compound **1** (R=H), a derivative of the amino acid methionine, might display a different coordination chemistry in Cu<sup>II</sup> and Cu<sup>I</sup> complexes (Scheme 1 and Fig. 1). The Cu<sup>II</sup> complex should coordinate the three nitrogen atoms and the carboxylate. For the (*S*)-enantiomer, this would result in negative chirality for the orientation of the chromophores and should give rise to a negative couplet in the ECCD spectrum. The Cu<sup>I</sup> complex, on the other hand, should show coordination by the dialkyl sulfide ligand in place of the carboxylate, which would invert the twist of the molecule, and yield a positive couplet in the ECCD spectrum. The inversion of the



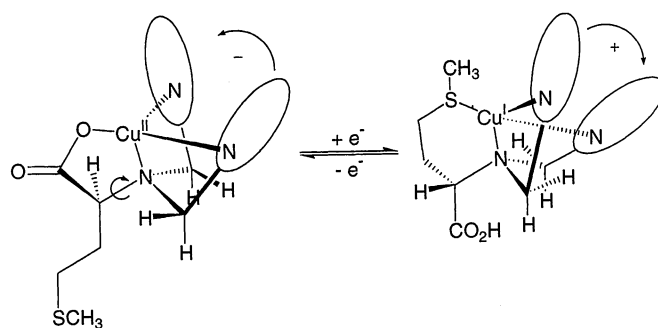
Scheme 1.

twist of the molecule would come about as a result of the pivoting of the amino acid arm about the C–N bond (Fig. 1), which would invert the direction of the C–H bond. This would in turn cause the other two methylene groups to rotate, resulting in inversion of the overall twist of the structure and therefore a change in chirality of the orientation of

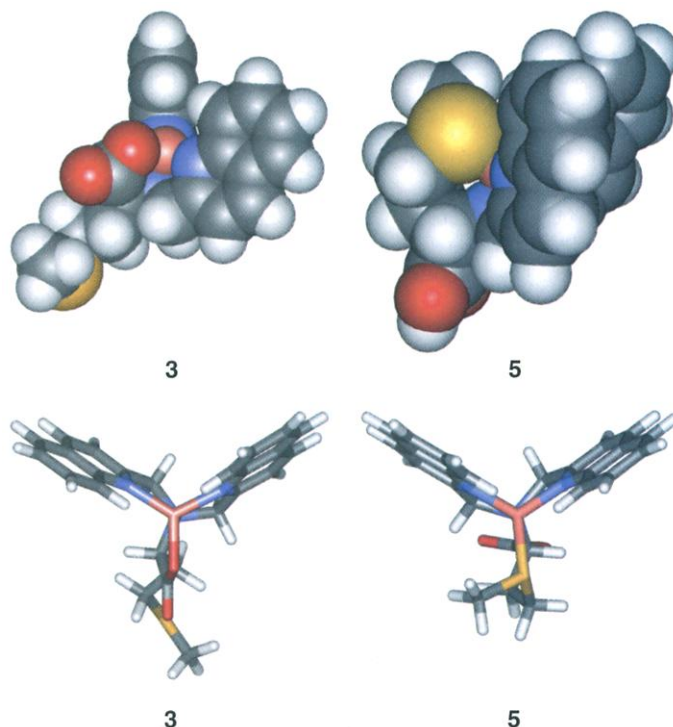
the quinoline chromophores with respect to one another. The two complexes are illustrated in Fig. 2 by structures calculated with semi-empirical methods. The side view shows the coordination of carboxylate in the Cu<sup>II</sup> complex and sulfide in the Cu<sup>I</sup> complex. The top view shows the twists of the two complexes as seen by opposite helicity of the synchronous C–H bonds and the opposite relative orientation of the planar quinoline moieties.

The metal complexes **3**, [Cu<sup>II</sup>(1H<sub>-1</sub>)]ClO<sub>4</sub>, and **4**, [Zn<sup>II</sup>(1H<sub>-1</sub>)]ClO<sub>4</sub>, gave elemental analyses consistent with proton loss from the carboxylate moiety (25). The ultraviolet-visible (UV-vis) spectrum showed Cu d-d transitions with absorbance maxima ( $\lambda_{\text{max}}$ ) at 725 and 810 nm, similar to other complexes that give ECCD spectra (18). The paramagnetic Cu<sup>II</sup> complex **3** could not be examined by

**Fig. 1.** Illustrated mechanism of conformational changes that occur upon reduction or oxidation of complexes. In the Cu<sup>II</sup> state, the carboxylate is coordinated to the metal, the three synchronous C–H bonds form a clockwise propeller, and the chromophores display negative chirality. In the Cu<sup>I</sup> complex, the carboxylate and sulfide donors are exchanged, causing inversion of the C–H twist and the chromophore orientational chirality.



**Fig. 2.** Graphic depictions of the two states of **3** and **5** [space filling in side view (top) and tube in top view (bottom)]. Structures were generated using molecular mechanics with MMFF94 force field followed by geometry optimization employing the semi-empirical method PM3/TM (SPARTAN software) (28).



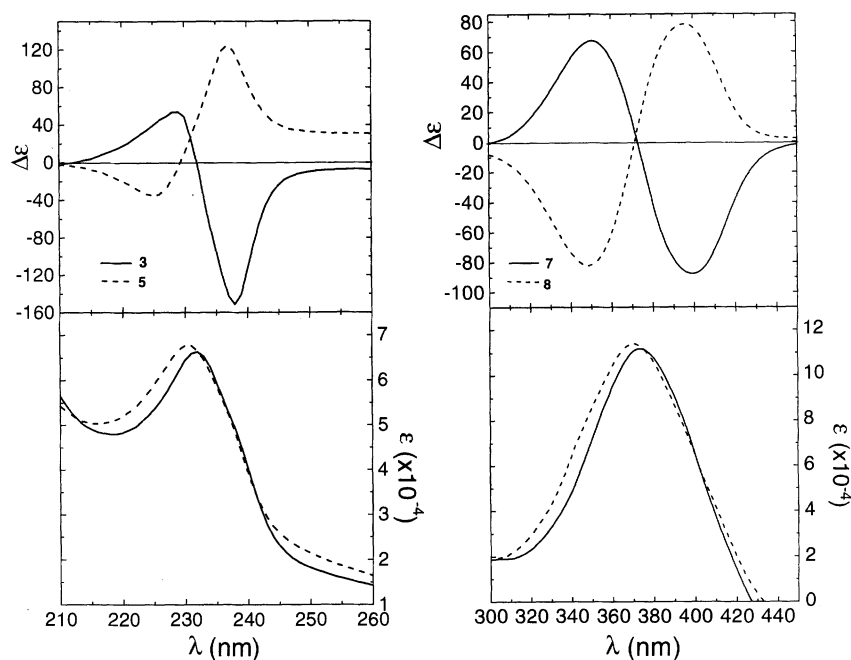


**Fig. 3.** CD (top) and absorption (bottom) spectra of copper complexes recorded in methanol (**3**, **5**) (left) and methylene chloride (**7**, **8**) (right) at 25°C. The split CD curve, the coincidence of the inflection point with the  $\lambda_{\max}$  of the low energy absorption band of the UV-vis spectra, and the large intensity of the signal are consistent with an exciton coupling mechanism. Isotropic ( $\epsilon$ ) and anisotropic ( $\Delta\epsilon$ ) extinction coefficient units are liters mol<sup>-1</sup> cm<sup>-1</sup>.

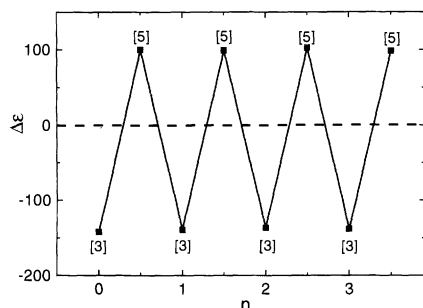


**Fig. 4.** Plot of  $\Delta\epsilon$  versus the number of cycles  $n$  at 239 nm in methanol, beginning with complex **3**.

nuclear magnetic resonance (NMR), so the geometrically analogous (*18*) Zn<sup>II</sup> complex **4** was examined. The <sup>1</sup>H NMR spectrum of the Zn<sup>II</sup> complex showed downfield shifts in resonances for protons near the tertiary amine atom but not for those near the sulfur atom, consistent with coordination of the carboxylate moiety, not the sulfide. In contrast, the Cu<sup>I</sup>PF<sub>6</sub> complex (**5**) of **1** gave a <sup>1</sup>H NMR spectrum with substantial downfield shift of the S-CH<sub>3</sub> group compared to the uncomplexed ligand, consistent with coordination of the sulfur atom to the metal ion. The elemental analysis of this complex fit the formula [Cu<sup>I</sup>(**1**)PF<sub>6</sub>], consistent with retention of the acidic proton and lack of coordination of the carboxylate to the metal ion.

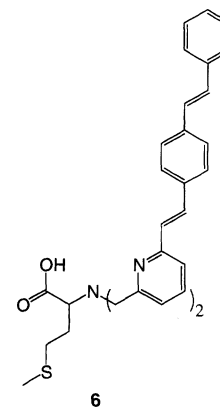
UV-vis and CD spectra of the two copper complexes **3** and **5** are shown in Fig. 3. The

UV-vis spectra are very similar, with a slight shift of  $\lambda_{\max}$  from 230 nm for the Cu<sup>I</sup> complex (**5**) to 232 nm for the Cu<sup>II</sup> complex (**3**), as also observed in earlier work with quinoline ligands. Both complexes show nonconservative ECCD spectra, with a reasonably large amplitude, couplets, and  $\Delta\epsilon = 0$  at 230 nm (**5**) and 232 nm (**3**) ( $\Delta\epsilon$  is the differential extinction coefficient for left and right circular polarized light). The two ECCD spectra are nearly mirror images of one another, differing only as a result of the slight shift in  $\lambda_{\max}$  for the electronic transition. Control experiments with the Cu<sup>I</sup> complex of ester **2** yielded an ECCD spectrum almost identical in shape and intensity to that of **5**, whereas the Cu<sup>II</sup> complex of **2** displayed a distorted spectrum of low intensity in comparison to that of **3**, as would be expected for the much weaker coordination of the ester compared with carboxylate.

The interconversion between the two oxidation states was observed to be reversible in solution (Fig. 4). Treatment of **3** with ascorbic acid resulted in a CD spectrum identical to that of **5**, whereas oxidation of **5** with ammonium persulfate produced the CD signal of **3** at room temperature (26). No hysteresis was observed after three complete cycles. Cyclic voltammetry (CV) studies of the complexes revealed a wide separation (0.9 V) between the anodic and cathodic peaks, as expected for conformational change of the ligand and exchange of the inner coordination sphere upon redox change. Variation of the scan rate did not affect the curve significantly, suggesting the absence of slow conforma-

tional interconversions, which must be much faster than the CV time scale. Cyclic voltammograms were reported for 20 cycles without a change in shape.

In an effort to achieve absorbance of a longer wavelength and to obtain ECCD spectra that are more conservative, we prepared the methionine derivative **6** (Scheme 2). This compound incorporates the stylyl-2-vinylpyridine chromophore, previously reported to show  $\lambda_{\max} = 359$  nm (isotropic extinction coefficient  $\epsilon = 60,000$ ) (27). The long-wavelength transition in this molecule was expected to show behavior similar to that of the transverse electronic transition of quinoline due to the similarity in the geometries of the transition dipole moments. UV-vis and ECCD spectra of **7**, [Cu<sup>II</sup>(**6H**<sub>-1</sub>)](ClO<sub>4</sub>)<sub>2</sub>, and **8**, [Cu<sup>I</sup>(**6**)PF<sub>6</sub>], are shown in Fig. 3. These spectra are very similar to the spectra ob-



**Scheme 2.**

served for the analogous complexes of **1** except that the curves exhibit more symmetry with respect to the null. The Cu<sup>II</sup> complex shows a negative couplet. The Cu<sup>I</sup> complex shows a positive couplet, corresponding to the positive orientation of the chromophores. This behavior is consistent with the conformations proposed for the respective complexes.

The redox-induced change of sign in the ECCD spectra results from inversion of the chromophoric exciton chirality. In these propeller-shaped molecules, this spectroscopic change is best rationalized by the inversion of the axial chiral element defined by the orientation of the two chromophores. In our model, the twist of the propeller is governed by steric factors emerging from the interactions of the amino acid part of the ligand that arise from the different binding preferences for the Cu<sup>II</sup>/Cu<sup>I</sup> couple in a well-defined complex.

#### References and Notes

- N. Koumura, R. W. J. Zijlstra, R. A. van Delden, N. Harada, B. L. Feringa, *Nature* **401**, 152 (1999).
- N. P. M. Huck, W. F. Jager, B. de Lange, B. L. Feringa, *Science* **273**, 1686 (1996).
- S. Z. Janicki and G. B. Schuster, *J. Am. Chem. Soc.* **117**, 8524 (1995).

4. M. Suarez and G. B. Schuster, *J. Am. Chem. Soc.* **117**, 6732 (1995).
5. S. Zahn and J. W. Canary, *Angew. Chem. Int. Ed. Engl.* **37**, 305 (1998).
6. L. Zelikovitch, J. Libman, A. Shanzer, *Nature* **374**, 790 (1995).
7. V. Goulle, A. Harriman, J. M. Lehn, *J. Chem. Soc. Chem. Commun.* **1993**, 1034 (1993).
8. S. Shinkai, K. Inuzuka, O. Miyazaki, O. Manbe, *J. Am. Chem. Soc.* **107**, 3950 (1985).
9. G. De Santis, L. Fabbri, M. Licchelli, P. Pallavicini, A. Perotti, *J. Chem. Soc. Dalton Trans.* **1992**, 3283 (1992).
10. N. Armaroli *et al.*, *J. Am. Chem. Soc.* **121**, 4397 (1999).
11. S. Muñoz and G. W. Gokel, *J. Am. Chem. Soc.* **115**, 4899 (1993).
12. P. R. Ashton *et al.*, *J. Am. Chem. Soc.* **121**, 3951 (1999).
13. C. Westermeier, H.-C. Gollmeier, J. Daub, *J. Chem. Soc. Chem. Commun.* **1999**, 2427 (1999).
14. M. Porsch, G. Sigl, *J. Daub, Adv. Mater.* **9**, 635 (1997).
15. D.-K. Yang, X.-Y. Huang, Y.-M. Zhu, *Annu. Rev. Mater. Sci.* **27**, 117 (1997).
16. C. Mao, W. Sun, Z. Shen, N. C. Seeman, *Nature* **397**, 144 (1999).
17. R. A. Bissell, E. Códova, A. E. Kaifer, J. F. Stoddart, *Nature* **369**, 133 (1994).
18. J. W. Canary, C. S. Allen, J. M. Castagnetto, Y. Wang, *J. Am. Chem. Soc.* **117**, 8484 (1995).
19. J. W. Canary *et al.*, *Enantiomer*, in press.
20. S. Zahn and J. W. Canary, *Org. Lett.* **1**, 861 (1999).
21. J. W. Canary *et al.*, *Inorg. Chem.* **37**, 6255 (1998).
22. J. M. Castagnetto, X. Xu, N. Berova, J. W. Canary, *Chirality* **9**, 616 (1997).
23. K. Nakanishi and N. Berova, in *Circular Dichroism: Principles and Applications*, K. Nakanishi, N. Berova, R. W. Woody, Eds. (VCH, New York, 1994), pp. 361–398.
24. Z. Tyeklár and K. D. Karlin, in *Bioinorganic Chemistry of Copper*, A. Tyeklár and K. D. Karlin, Eds. (Chapman & Hall, New York, 1993), pp. 277–291.
25. Ligands **1** and **2** were synthesized by the alkylation of L-methionine or its methyl ester with two equivalents of 2-bromomethylquinoline in the presence of NaHCO<sub>3</sub> in dimethylformamide. Ligand **5** was prepared from stilbene-4-carboxaldehyde, which was reacted with the mono-triphenylphosphonium salt of 2,6-dibromomethylpyridine to yield 6-bromomethyl-2-vinyl-stilbenyl pyridine. The alkylation of methionine was carried out similar to that of **2**. All new compounds were characterized by standard spectroscopic means and gave satisfactory elemental analysis.
26. In a typical experiment, 0.35 ml of a 0.3 mM solution of **3** was placed in a 1-mm pathlength cell. After recording the CD spectrum, 0.011 ml of a 10 mM solution of ascorbic acid was added to the solution, and another CD spectrum was recorded. Adding 0.011 ml of a 10 mM solution of ammonium persulfate and recording the CD spectrum completed one cycle.
27. A. E. Siegrist, H. R. Meyer, P. Gassman, S. Moss, *Helv. Chim. Acta* **63**, 1311 (1980).
28. SPARTAN 5.1, Wavefunction, Inc., Irvine, CA.
29. We thank H. Barcena and J. McBride for help with electrochemical measurements. This work was supported by NIH grant GM49170.

30 November 1999; accepted 5 April 2000

## Quantifying Denitrification and Its Effect on Ozone Recovery

A. Tabazadeh,<sup>1\*</sup> M. L. Santee,<sup>2</sup> M. Y. Danilin,<sup>3</sup> H. C. Pumphrey,<sup>4</sup> P. A. Newman,<sup>5</sup> P. J. Hamill,<sup>6</sup> J. L. Mergenthaler<sup>7</sup>

Upper Atmosphere Research Satellite observations indicate that extensive denitrification without significant dehydration currently occurs only in the Antarctic during mid to late June. The fact that denitrification occurs in a relatively warm month in the Antarctic raises concern about the likelihood of its occurrence and associated effects on ozone recovery in a colder and possibly more humid future Arctic lower stratosphere. Polar stratospheric cloud lifetimes required for Arctic denitrification to occur in the future are presented and contrasted against the current Antarctic cloud lifetimes. Model calculations show that widespread severe denitrification could enhance future Arctic ozone loss by up to 30%.

Polar stratospheric clouds (PSCs) play important roles in the formation of the springtime Antarctic “ozone hole” by activating chlorine and denitrifying the stratosphere (1–7). Although similar abundances of reactive chlorine have been measured in both polar vortices (8–12), ozone loss has typically been much less severe over the Arctic than over the Antarctic (1, 2). The Arctic vortex has generally been warmer, weaker, less persistent, and more distorted than the Antarctic vortex (13, 14), and consequently up to now the Arctic has been less susceptible to ozone depletion. Although there has been signifi-

cant ozone loss in the Arctic, especially in the coldest winters of the last decade (1, 2, 15–19), the magnitude of such loss has been partially masked by transport of ozone-rich air from higher altitudes (16–21). It has been suggested (6, 7) that the observed lack of widespread severe denitrification in the Arctic (22–24) may be a major factor currently preventing the formation of an Arctic “ozone hole.”

Here, the concept of “PSC lifetime” is introduced to explore how long a PSC must persist in the winter for denitrification to occur, and why the event currently occurs in the Antarctic but not in the Arctic. “PSC lifetime” is defined as the average time an air mass is exposed to temperatures below the condensation point of thermodynamically known solid PSC particle phases, such as nitric acid trihydrate (NAT), nitric acid dihydrate (NAD), and ice.

Some studies have implied that Arctic denitrification has contributed to ozone depletion inside the Arctic vortex during the coldest winters of the last decade (15, 25). Others (26–31) suggest that simultaneous loss of ozone and reactive nitrogen in the

Arctic is often a result of dynamical mixing of different air masses and is unrelated to denitrification. Also, most in situ and balloon data sets (25, 32–36) showing denitrification in the Arctic were collected near mountainous terrain, where lee waves could have strongly affected the local reactive nitrogen (37) [or water vapor (38)] profile through small-scale cloud processing. Overall, the fact that satellite data (22–24) show no indication of widespread denitrification in the Arctic at present may suggest that the local perturbations caused by lee waves are not of global or regional significance, in terms of leading to a substantial irreversible removal of nitric acid vapor. However, lee wave-generated PSCs may still play a role in Arctic ozone depletion by providing additional surface areas upon which chlorine activation can occur (39).

Here we examine both denitrification and dehydration of the Antarctic polar vortex in 1992 by correlating the depletion in nitric acid (40) and water vapor (41) concentrations, measured by Microwave Limb Sounder (MLS), with the increase in aerosol extinction (42) measured by Cryogenic Limb Array Etalon Spectrometer (CLAES). To identify the onset and duration of denitrification and dehydration in the Antarctic, we generated daily maps of gas phase nitric acid, water vapor, and aerosol extinction for different potential temperature surfaces from early May through November. Figure 1 shows daily polar maps for selected dates during the Antarctic winter of 1992 interpolated onto the 450 K potential temperature surface. A denitrified or dehydrated region is defined as an area in which nitric acid or water vapor mixing ratios, as seen by MLS, are depleted below 2 parts per billion by volume (ppbv) and 3 parts per million by volume (ppmv), respectively, without a significant corresponding increase in aerosol extinction, indicating the absence of solid nitric acid or ice PSCs.

Before 12 June, the PSCs that formed

<sup>1</sup>NASA Ames Research Center, MS 245-4, Moffett Field, CA 94035-1000, USA. <sup>2</sup>NASA Jet Propulsion Laboratory, MS 183-701, Pasadena, CA 91109, USA. <sup>3</sup>Atmospheric and Environmental Research, Inc., 840 Memorial Drive, Cambridge, MA 02139-3794, USA. <sup>4</sup>Department of Meteorology, University of Edinburgh, Mayfield Road, Edinburgh, EH9 3JZ Scotland. <sup>5</sup>NASA Goddard Space Flight Center, Code 916, Greenbelt, MD 20904, USA. <sup>6</sup>Department of Physics, San Jose State University, One Washington Square, San Jose, CA 95192, USA. <sup>7</sup>Lockheed Martin Advanced Technology Center, 3251 Hanover Street, Palo Alto, CA 94304, USA.

\*To whom correspondence should be addressed. E-mail: atabazadeh@mail.arc.nasa.gov